SAND2007-4988C

Heterogeneous Dynamic Behavior and Failure of a Tungsten Alloy: Experiments and Simulations

Tracy J. Vogler
Solid Dynamics and Energetic Materials Department
Sandia National Laboratories

&

John D. Clayton
Impact Physics Branch
U.S. Army Research Laboratory

ASME Applied Mechanics and Materials Conference
Austin, Texas
June 6, 2007

Sandia is a multiprogram laboratory operated by Sandia Corporation, a Lockheed Martin Company, for the United States Department of Energy's National Nuclear Security Administration under contract DE-AC04-94AL85000.

Introduction - WHA

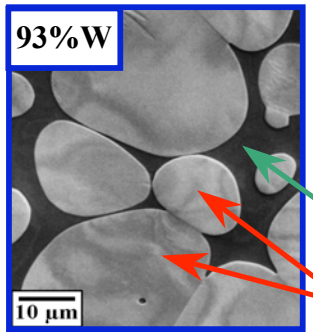

WHA =
Tunsten (**W**) **H**eavy **A**lloy
17.8 g/cm^3

tungsten-nickel-iron matrix

tungsten crystals

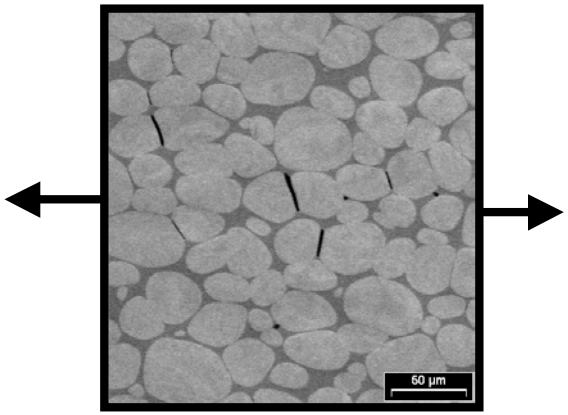

Local failure modes

- Shear bands
- Fracture at grain-grain & matrix-grain interface

EBSD: Tony Rollett (CMU)

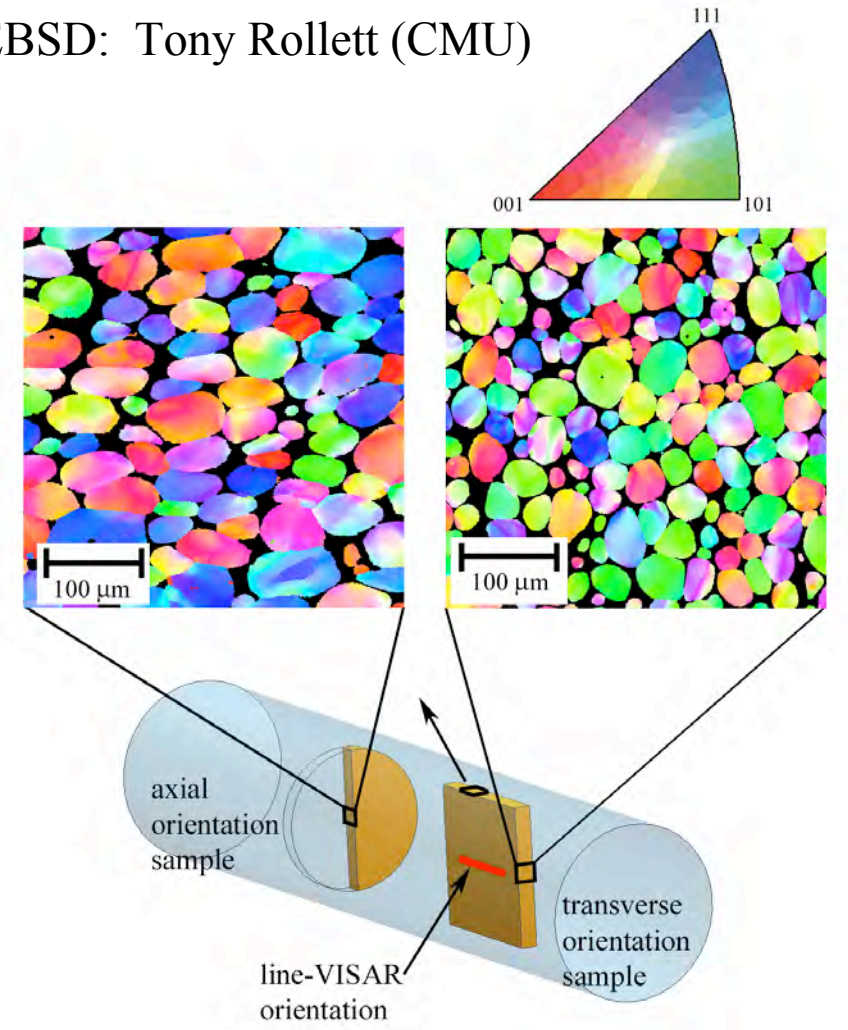

Single crystal ballistic tests suggest important role of texture

Plate Impact with Gas Guns

gas guns

- launch thin plates at high velocities
- provide well-posed initial conditions
- sample is in uniaxial ***strain***
- used to study material behavior at high pressures and strain rates

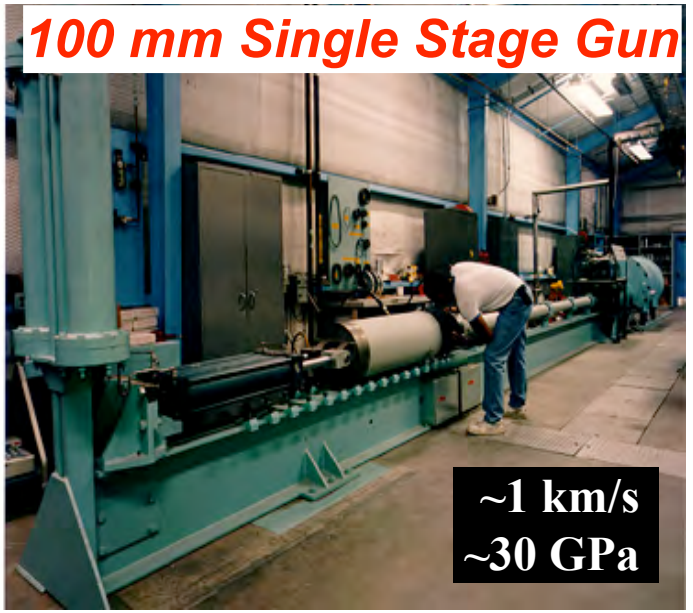

compressed helium used to launch projectiles as fast as 1 km/s

What is Spall?

- spall is dynamic tensile failure of a material due to interactions of waves
- failure initiates at internal flaws (triple points, voids, inclusions, etc.) rather than surface flaws
- spall strengths are typically much higher than tensile strengths measured in quasi-static experiments
- spall experiments typically involve plate impact experiments with dimensions of 1:2 for impactor and target

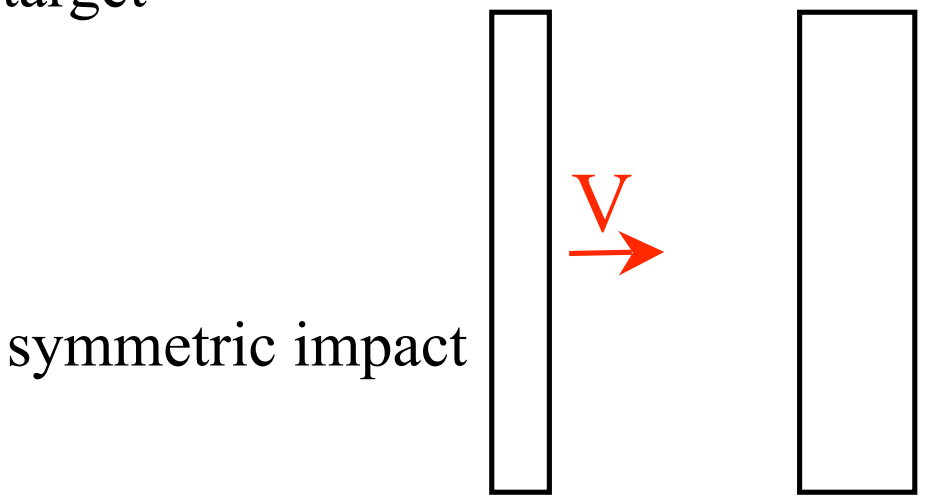

A Spall Experiment

- impactor hits stationary target at t = 0

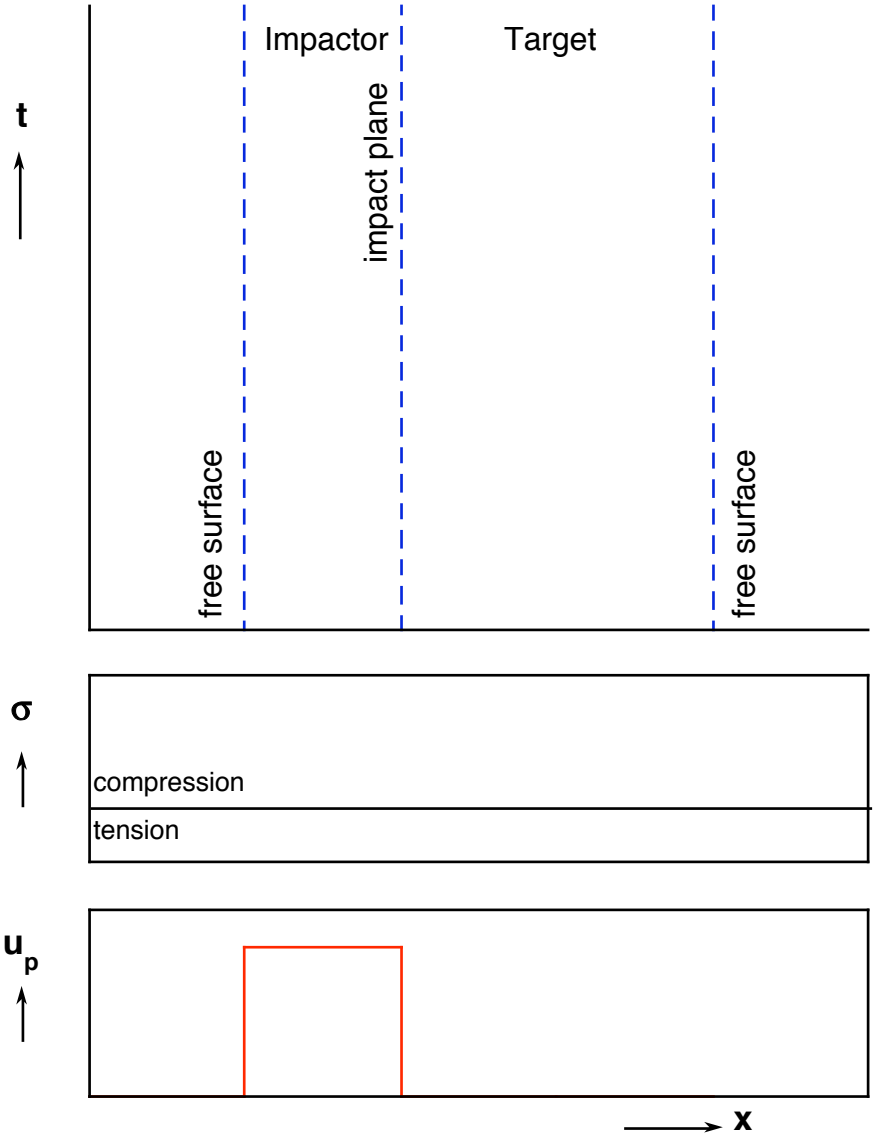

A Spall Experiment

- impactor hits stationary target at t = 0
- shocks travel into impactor and target

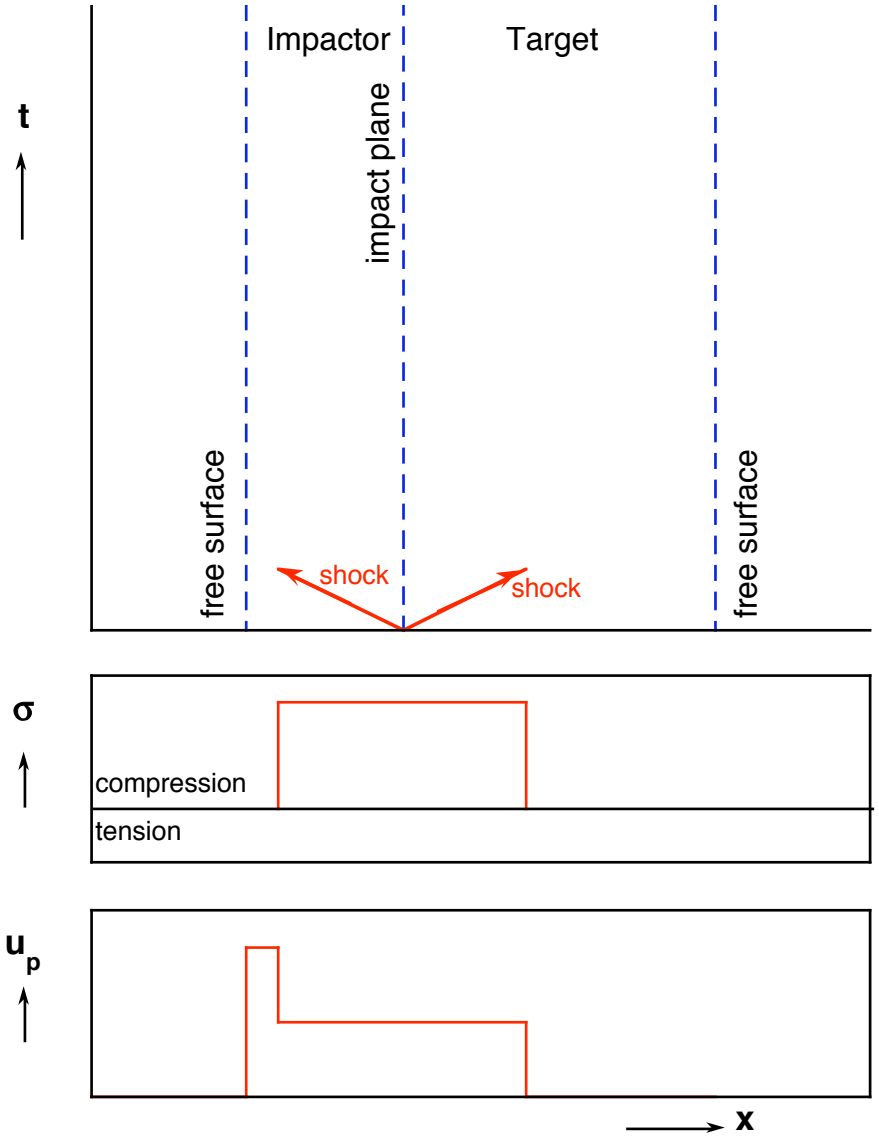

A Spall Experiment

- impactor hits stationary target at t = 0
- shocks travel into impactor and target
- shock in impactor reflects from free surface as release (unloading) wave (rarefaction fan)

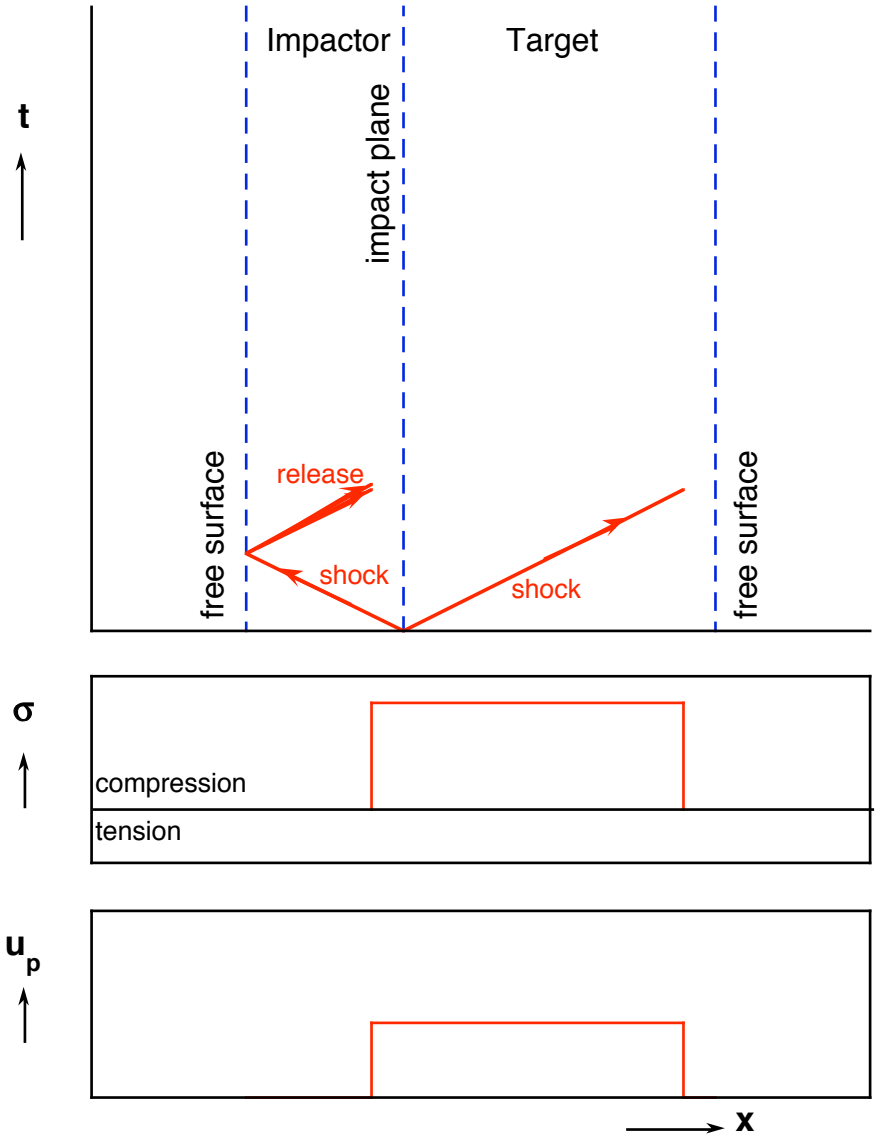

A Spall Experiment

- impactor hits stationary target at t = 0
- shocks travel into impactor and target
- shock in impactor reflects from free surface as release (unloading) wave (rarefaction fan)
- same thing happens in target

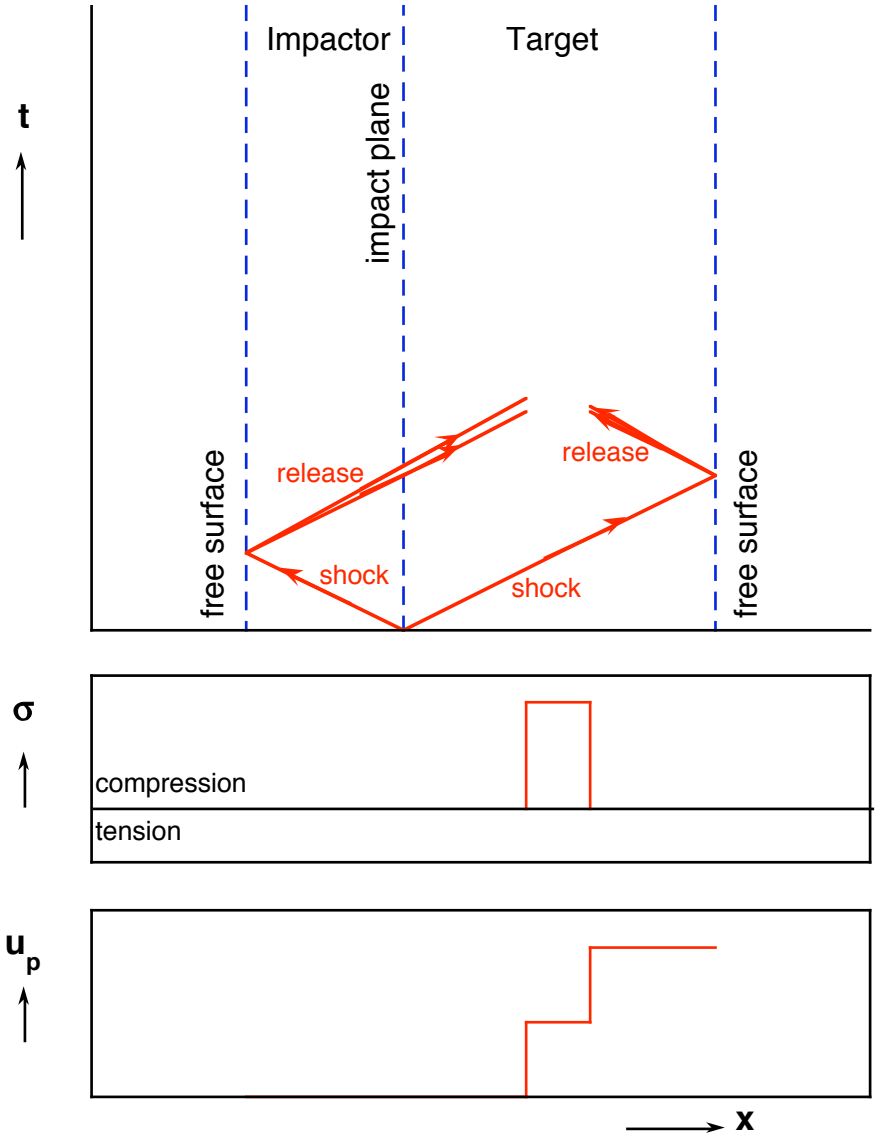

A Spall Experiment

- impactor hits stationary target at t = 0
- shocks travel into impactor and target
- shock in impactor reflects from free surface as release (unloading) wave (rarefaction fan)
- same thing happens in target
- release waves intersect at mid-plane and cause tensile stresses to build

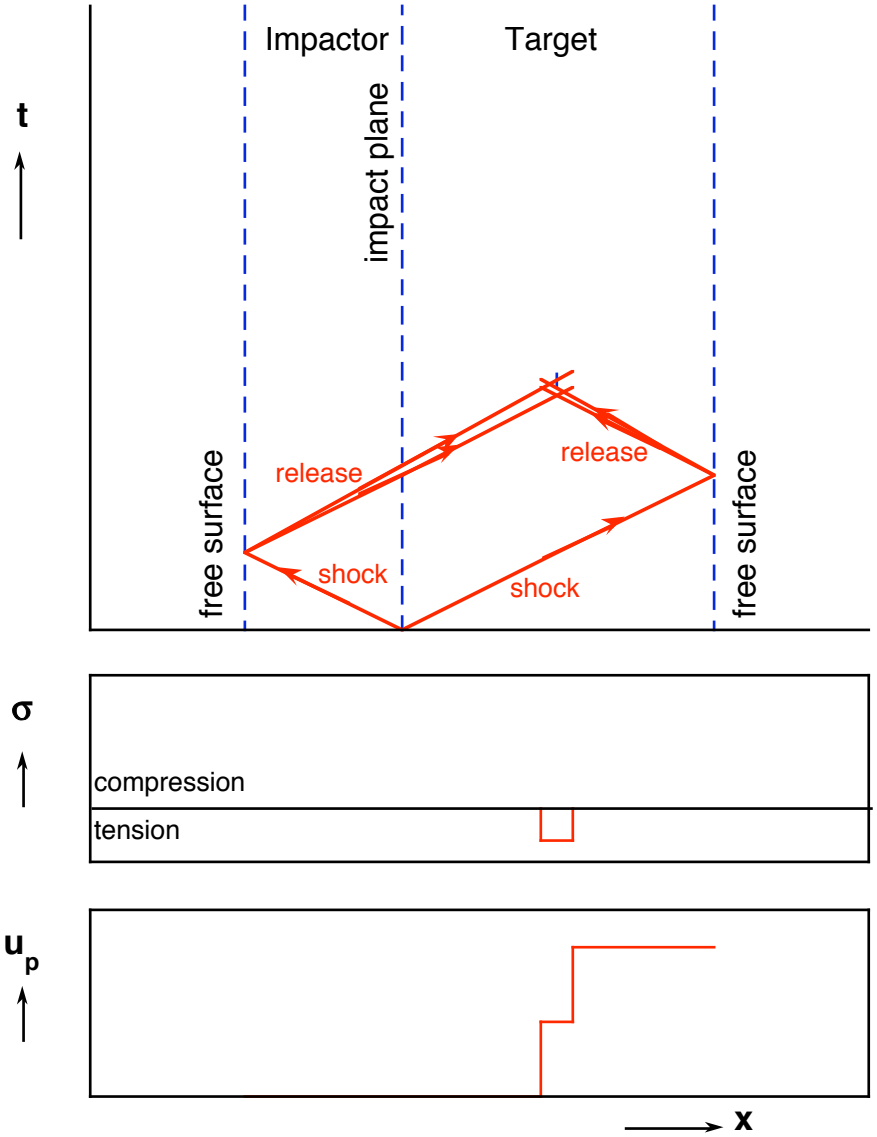

A Spall Experiment

- impactor hits stationary target at t = 0
- shocks travel into impactor and target
- shock in impactor reflects from free surface as release (unloading) wave (rarefaction fan)
- same thing happens in target
- release waves intersect at mid-plane and cause tensile stresses to build
- if stresses are large enough, sample fails in tension and spall plane forms

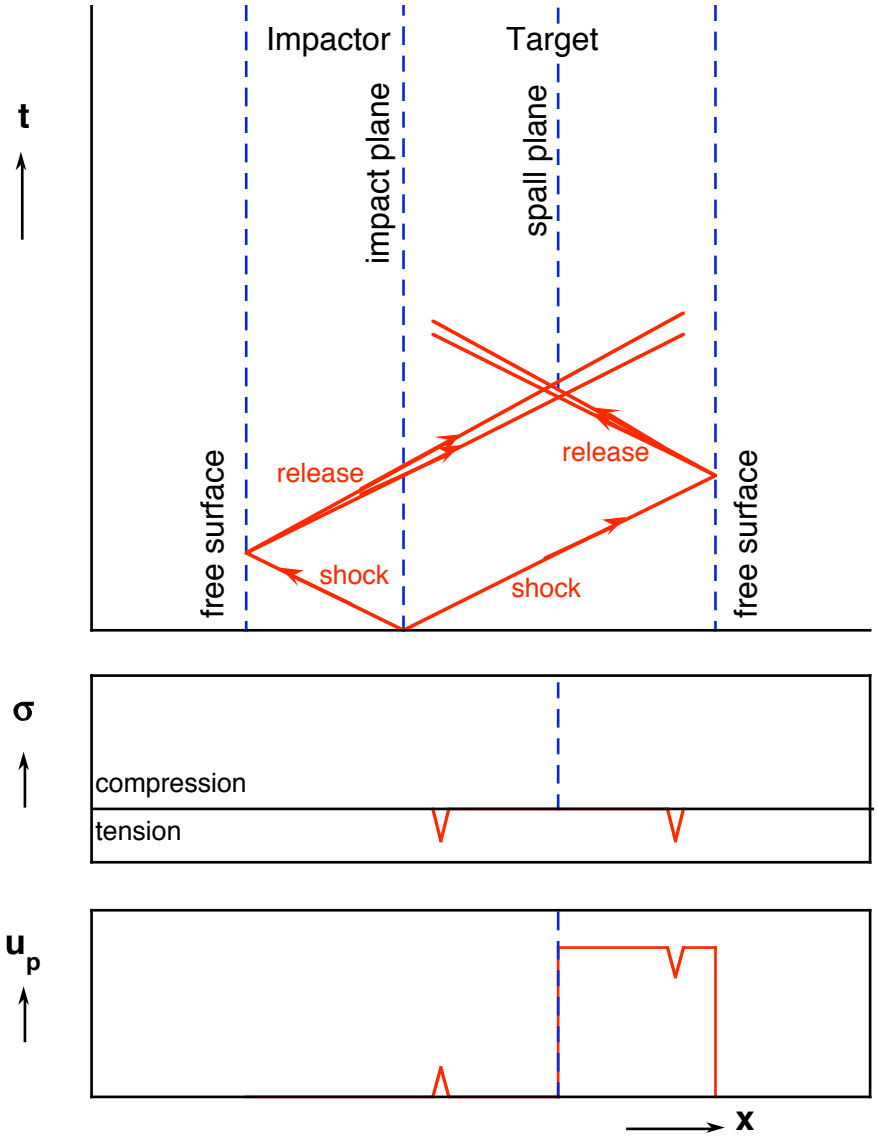

A Spall Experiment

- impactor hits stationary target at t = 0
- shocks travel into impactor and target
- shock in impactor reflects from free surface as release (unloading) wave (rarefaction fan)
- same thing happens in target
- release waves intersect at mid-plane and cause tensile stresses to build
- if stresses are large enough, sample fails in tension and spall plane forms
- sample separates at spall plane; waves continue to “ring” in spalled sample

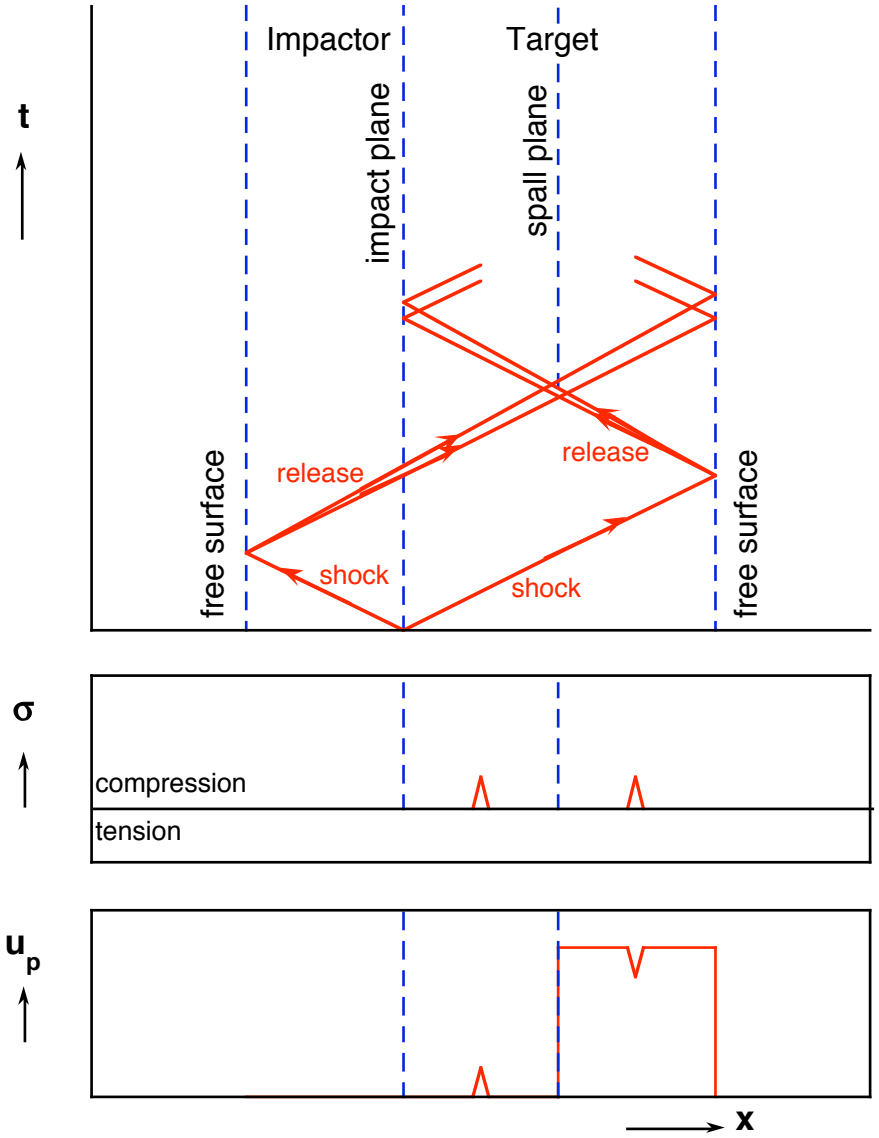

Background: VISAR Diagnostics

Velocity Interferometer System for Any Reflector (VISAR) [Barker & Hollenbach, 1972] uses Doppler shift to measure free surface velocity history during spall experiment

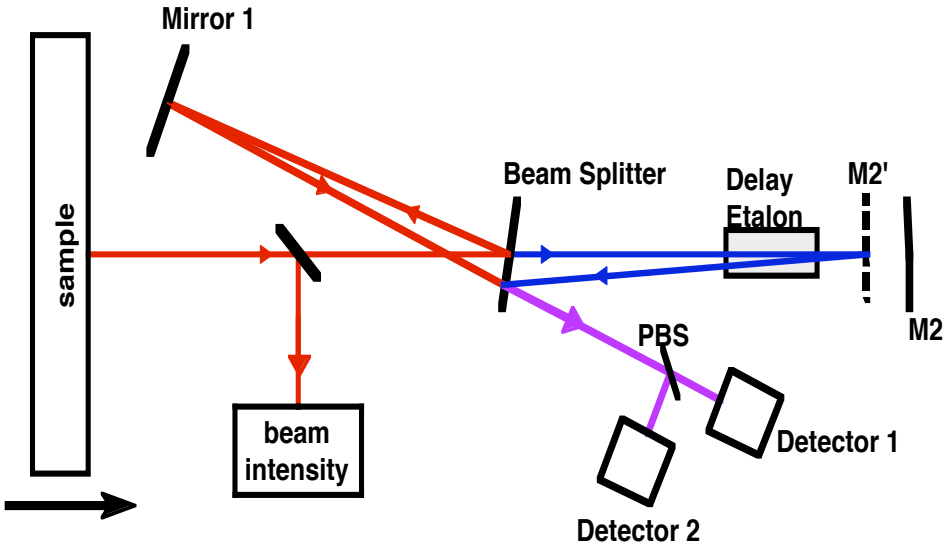

single point measurement, typically 50-200 μm

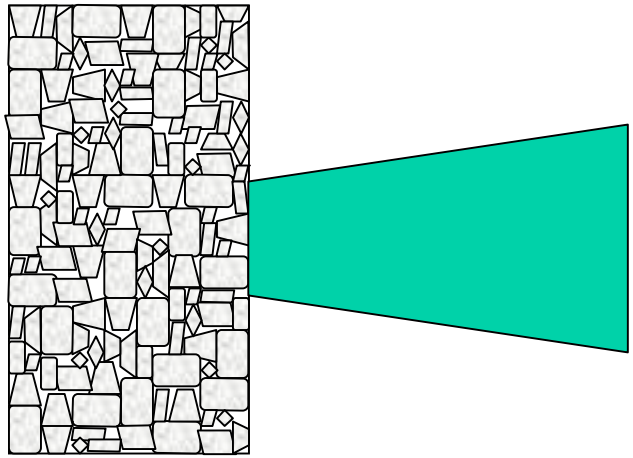

heterogeneity within the spot diameter averaged; no information outside this region

Background: Line-VISAR

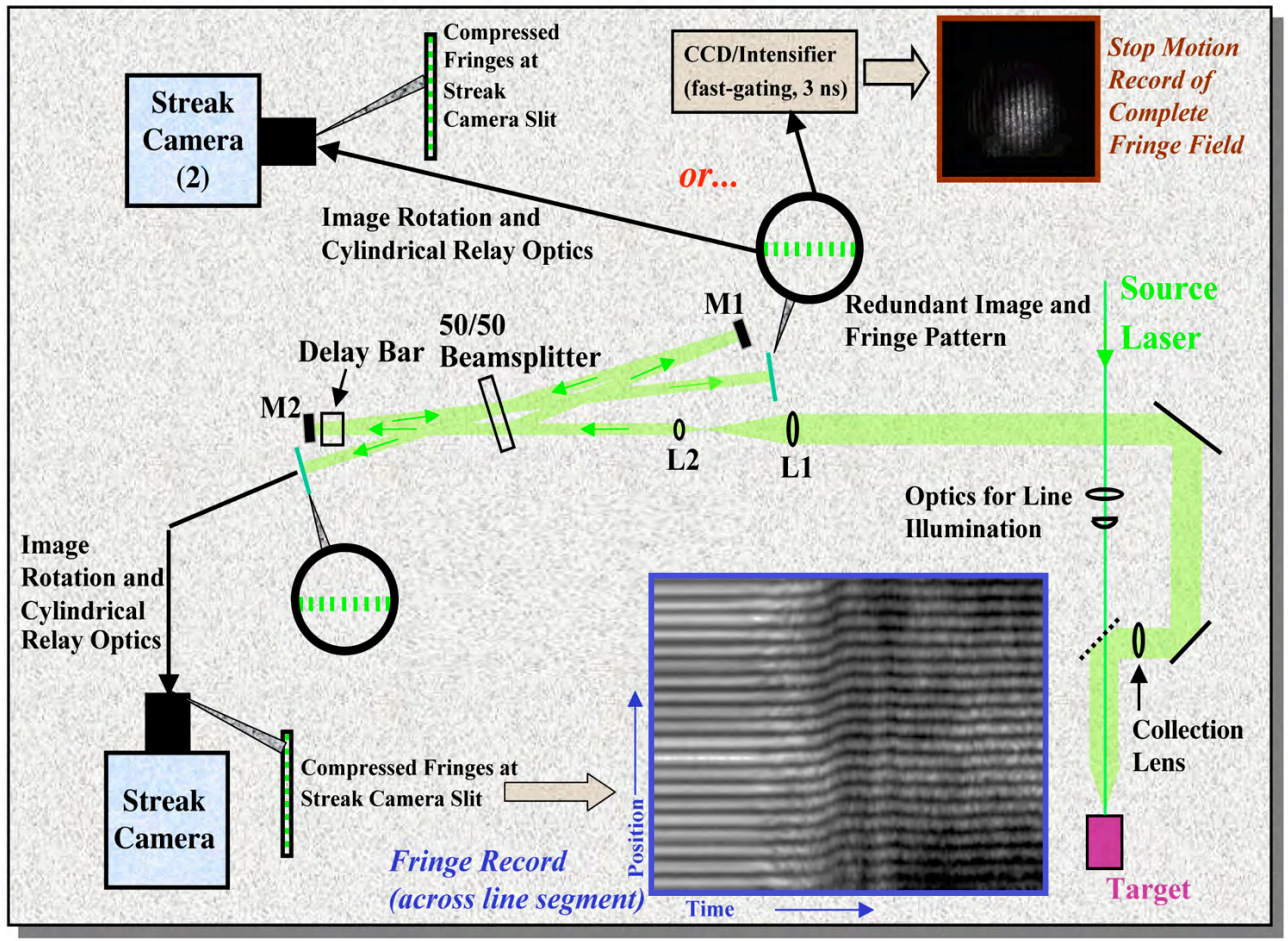

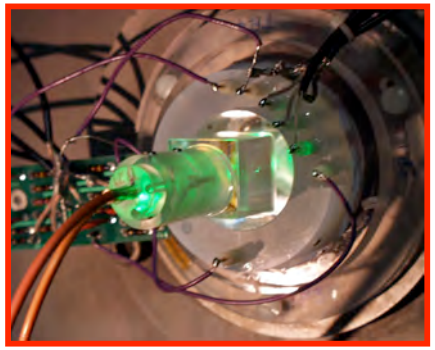

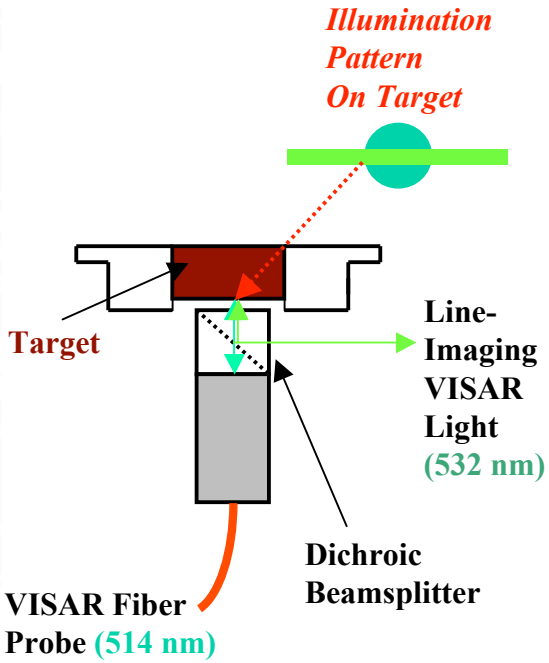

resolution as high as ~10 μm can be achieved along the line
only way to resolve this scale in dynamic experiments

Streak Camera Record

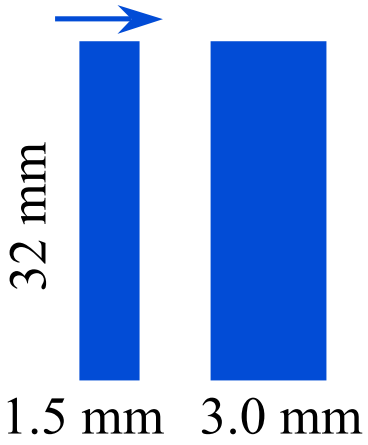

WHA-2

V = 345 m/s, σ = -13.4 GPa

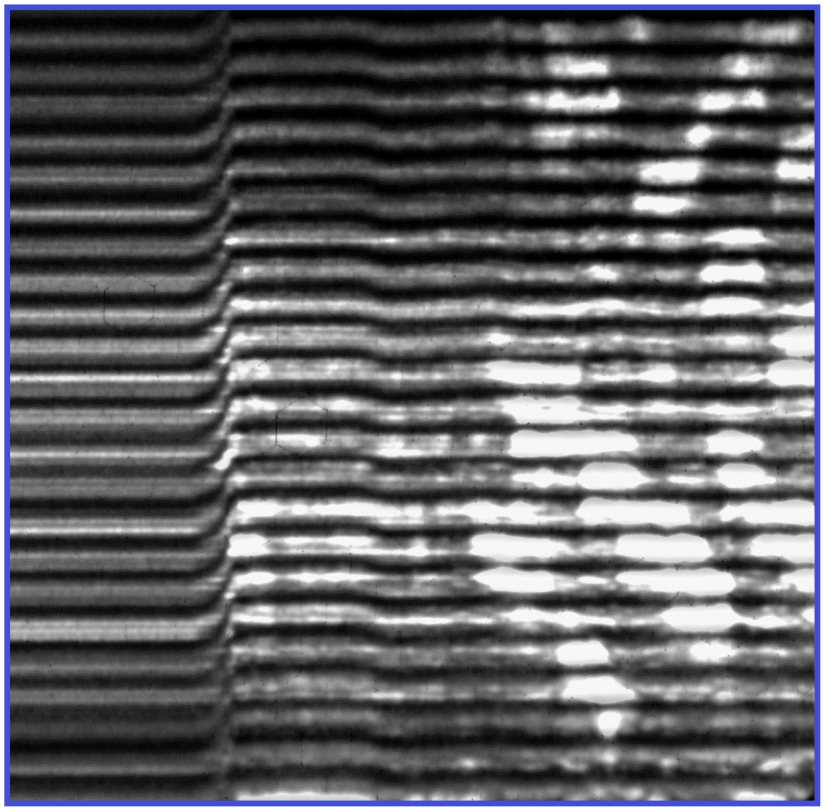

Longitudinal Section

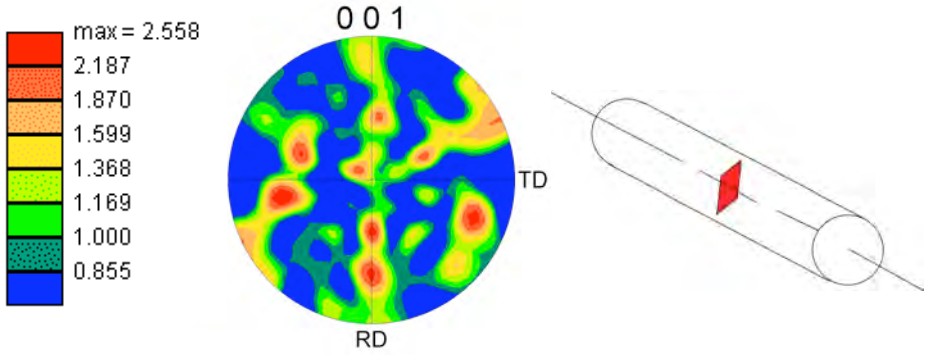

WHA-2 Results

Impact Velocity = 345 m/s

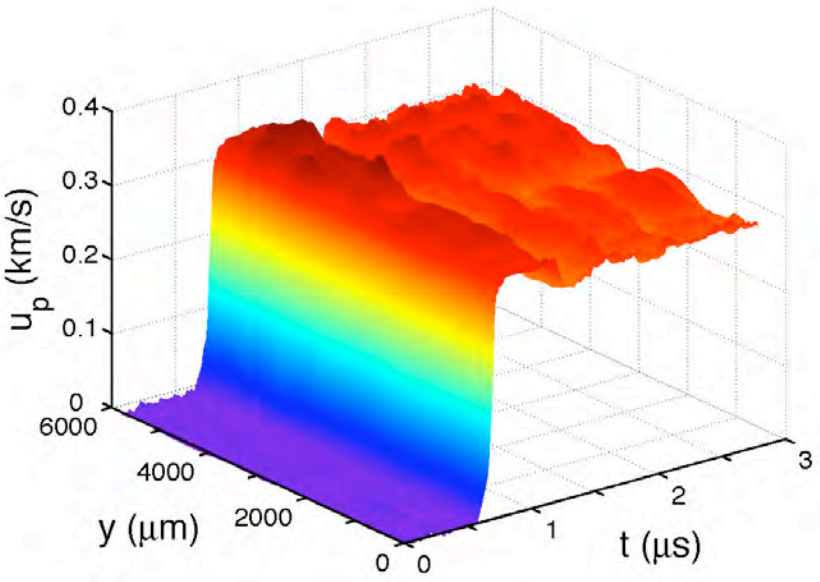

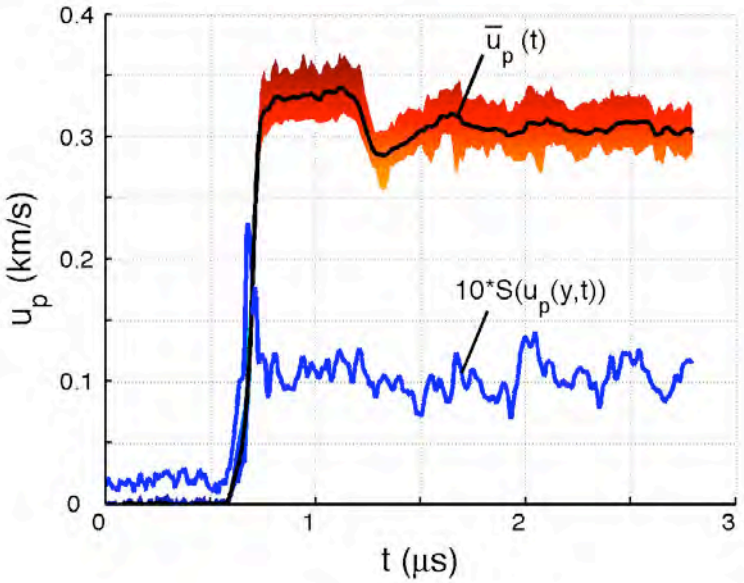

- velocity fluctuations spaced 100-1000 microns (larger than grain size)
- average response similar to previous point VISAR results
- deviations nearly constant except at shock front at around 3% of mean
- period for shock arrival approximately 1 mm

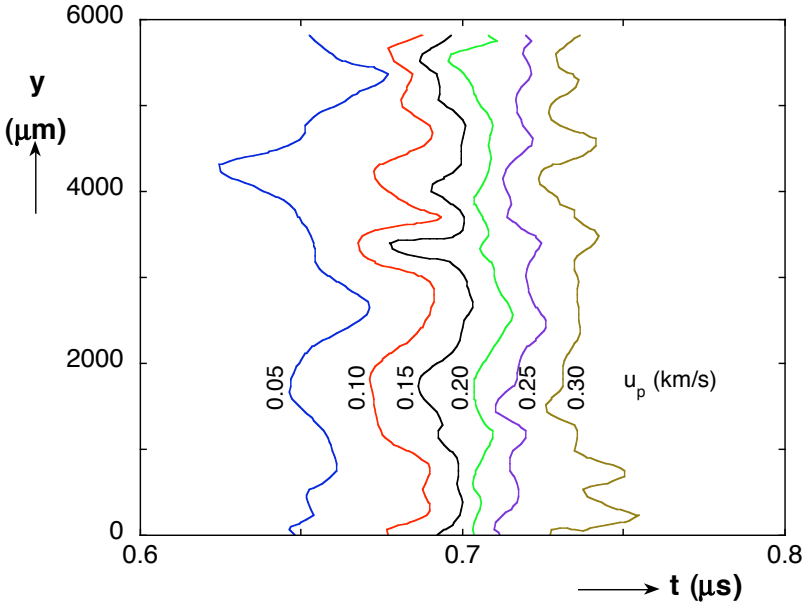

Results for Different Orientations and Velocities

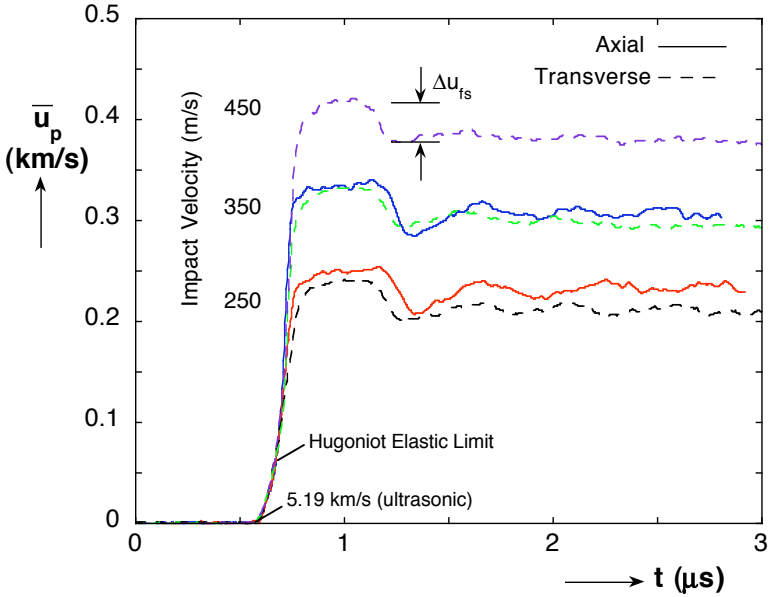

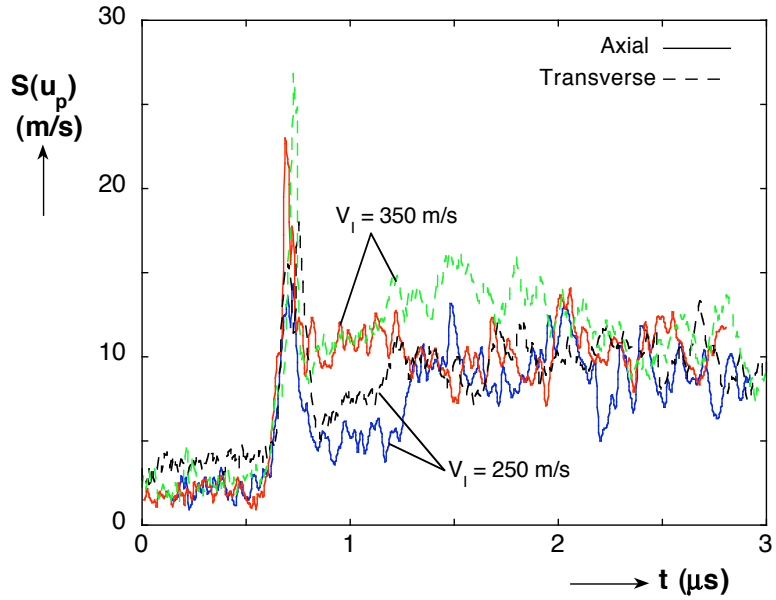

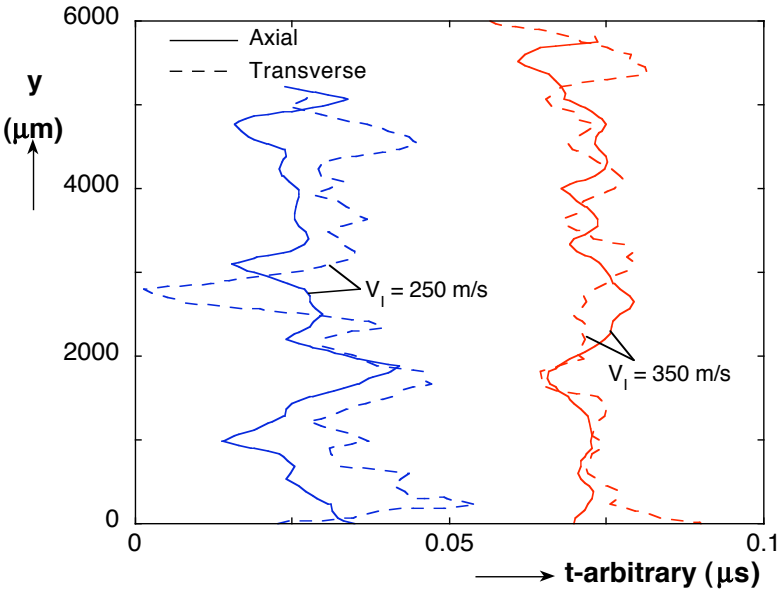

- transverse response slightly softer
- ringing in spalled material less pronounced for transverse samples
- higher impact velocities give somewhat higher deviations but no apparent correlation with microstructure
- wave fronts rougher for lower velocities (ratio ~0.6) and for transverse vs. axial samples (ratio ~0.6)

Distributions of Spall Strengths

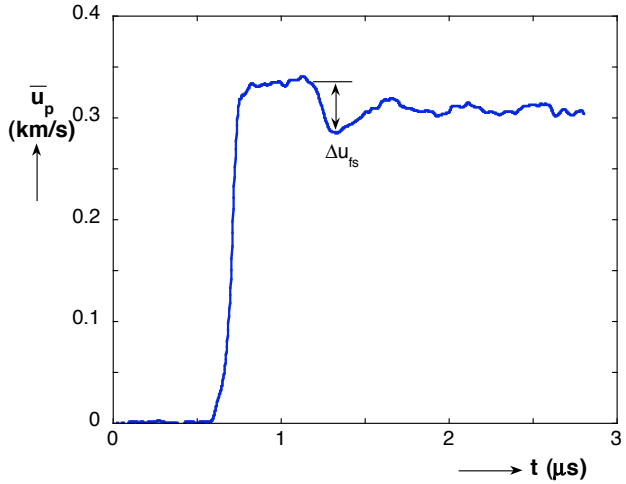

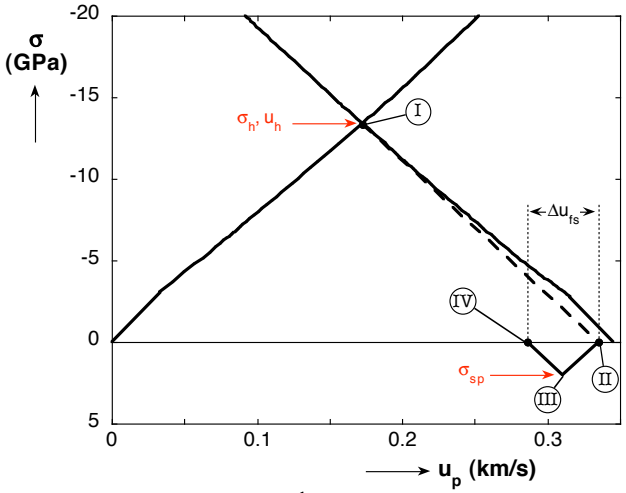

$$\sigma_{sp} \approx \frac{1}{2}\rho_o U_t \Delta u_{fs}$$

(assuming plane waves)

- significant variation in spall strengths for a given experiment
- average strengths 0.2-0.4 GPa higher for axial
- strength increases with impact velocity
- both Weibull and normal distributions fit data
- Weibull modulus 5-7 for all experiments (slightly higher for axial samples)

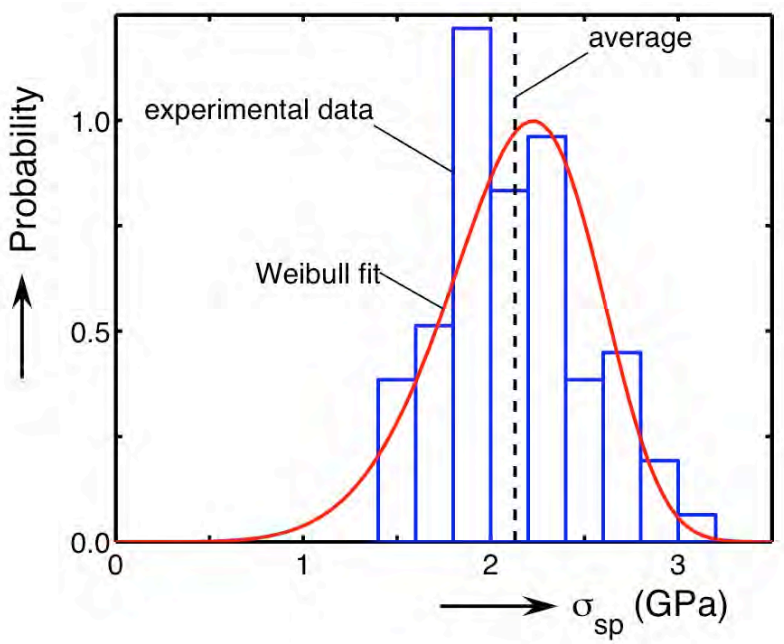

Crystal Plasticity Modeling

finite crystalline thermoelastic-viscoplastic framework

$$\mathbf{f} \equiv \partial \mathbf{x} / \partial \mathbf{X} = \mathbf{f}^{\mathrm{e}} \mathbf{f}^{\grave{\mathrm{e}}} \mathbf{f}^{\mathrm{p}}$$

Kinematics: $\mathbf{l}^{\grave{\mathrm{e}}} = \dot{\mathbf{f}}^{\grave{\mathrm{e}}} \mathbf{f}^{\grave{\mathrm{e}}-1} = \alpha_T \dot{\theta} \mathbf{1}$

$$\overline{\mathbf{l}}^{\mathrm{p}} \equiv \dot{\mathbf{f}}^{\mathrm{p}} \mathbf{f}^{\mathrm{p}-1} = \sum_{\alpha=1}^{n} \dot{\gamma}^{(\alpha)} \mathbf{s}_0^{(\alpha)} \otimes \mathbf{m}_0^{(\alpha)}$$

Flow rule: $\dot{\gamma}^{(\alpha)} = \dot{\gamma}_0 \left(\tilde{\tau}^{(\alpha)} / g^{(\alpha)} \right)^m \operatorname{sgn}\left(\tilde{\tau}^{(\alpha)} \right)$

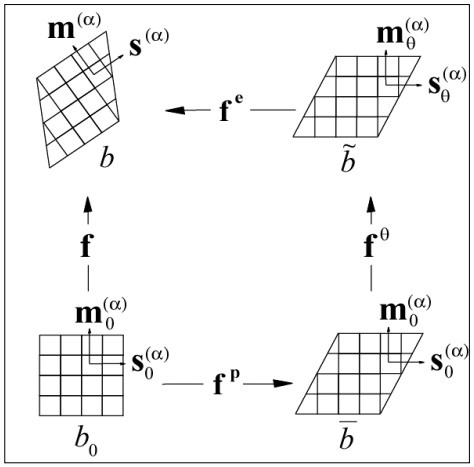

Free energy: $\tilde{\rho}\psi = \frac{1}{2} K_0(\theta)\vartheta^2 - \frac{1}{3} K_1 \vartheta^3 + \mu(\theta)\mathbf{e}^{\mathbf{e}'} : \mathbf{e}^{\mathbf{e}'} + \frac{1}{2}\kappa\mu(\theta)\xi^2 + y(\theta)$

Energy balance: $\underbrace{\rho \hat{c} \dot{\theta}}_{\text{temperature change}} = \underbrace{\sum_{\alpha=1}^{n} \tau^{(\alpha)} \dot{\gamma}^{(\alpha)}}_{\text{plastic dissipation}} \underbrace{- \rho \left(\left(\partial_\xi \psi \right) - \theta \left(\partial_{\theta\xi} \psi \right) \right) \dot{\xi}}_{\text{energy of lattice defects}} + \underbrace{\rho \theta \partial_{\theta \mathbf{e}^{\mathrm{e}}} \psi : \dot{\mathbf{e}}^{\mathrm{e}}}_{\text{thermoelastic coupling}} + \underbrace{div\left(k \nabla_{\mathbf{x}} \theta \right)}_{\text{heat conduction}}$

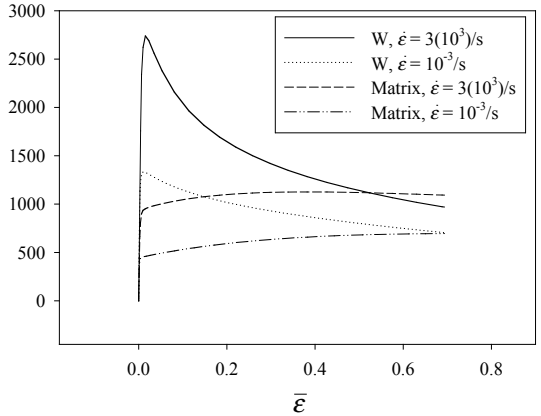

Stress-strain response for 300 random grains
(uniaxial compression, Taylor constraints)

- 24 slip systems for BCC W grains
- 12 slip systems for FCC matrix
- properties inferred from literature, mainly from static and intermediate rate experiments

Clayton, J.D., *J. Mech. Phys. Solids* **53**, 2005.
Clayton, J.D., *Int. J. Solids Structures* **42**, 2005.

Microstructure Representation

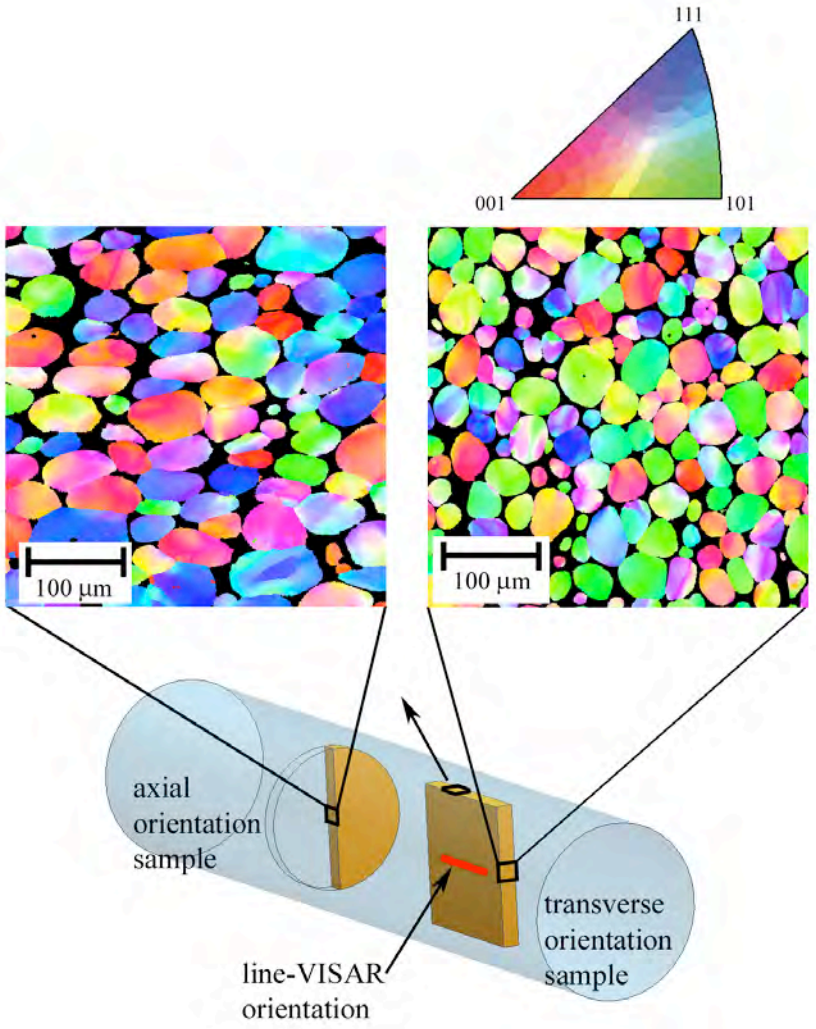

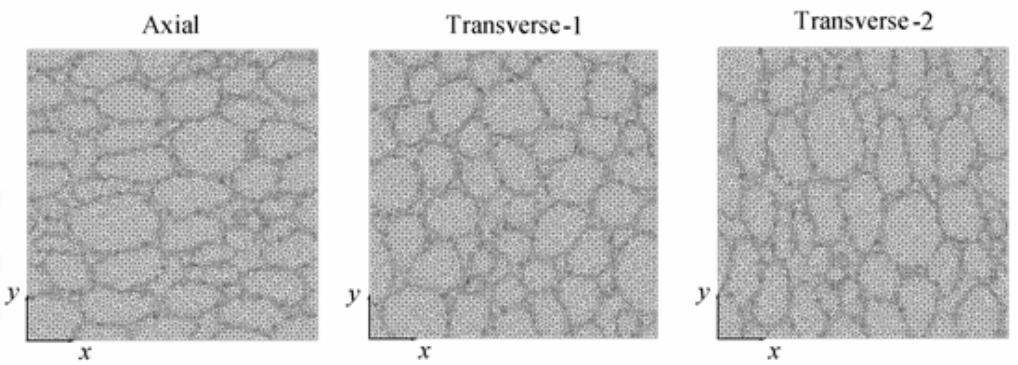

- Realistic grain shapes, sizes, volume fractions, and lattice orientations
- plane strain
- rigid upper and lower boundaries

WHA-I	axial	350 m/s
WHA-II	transverse-1	350 m/s
WHA-III	transverse-2	250 m/s
WHA-IV	transverse-2	350 m/s
WHA-V	transverse-1	450 m/s

Fracture Modeling: cohesive approach

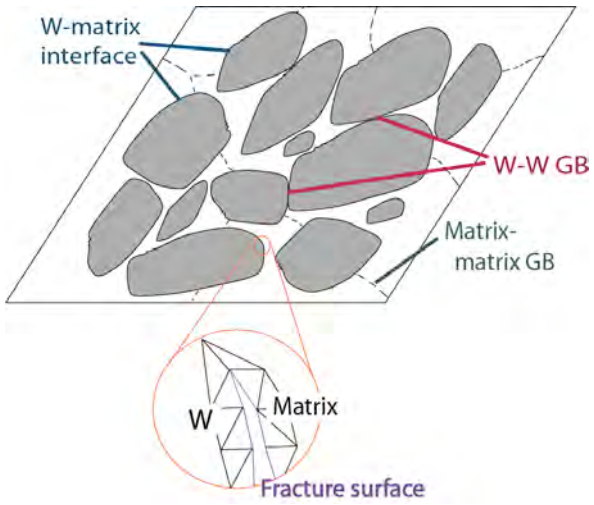

- new crack surfaces generated via traction criteria at interfaces (Camacho & Ortiz, 1996)
- focus on **intergranular fracture** at W-W and W-matrix interfaces
- nominal fracture properties: **fracture stress** (300K) (**Dandekar & Weisgerber**, 1999; **Weerasooriya**, 2003; **Bjerke**, 2004)

$$\hat{s}_0 = 2.0 \text{ GPa}$$

- **fracture toughness** (compromise of values from literature)

$$K_{Ic} = \sqrt{G_c E/(1-\nu^2)} = 20 \text{ MPa}\sqrt{\text{m}}$$

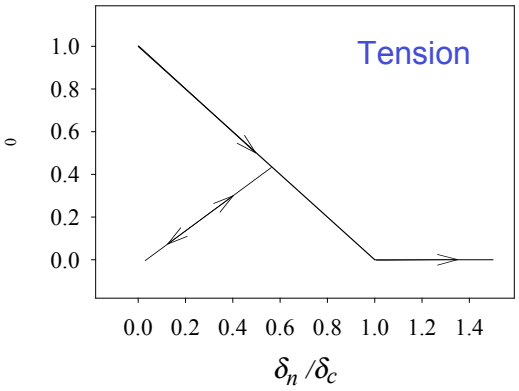

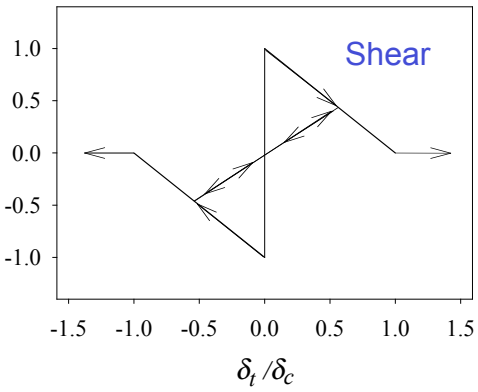

$r = 70$ μm (2 W-grain diameters)

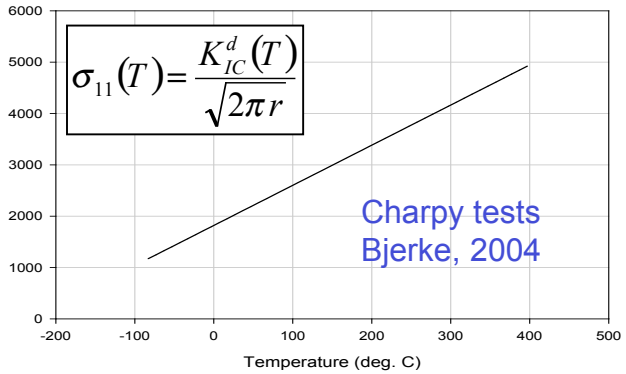

- cleavage could be important, not modeled here

Model results: WHA-IV

transverse-2, 350 m/s

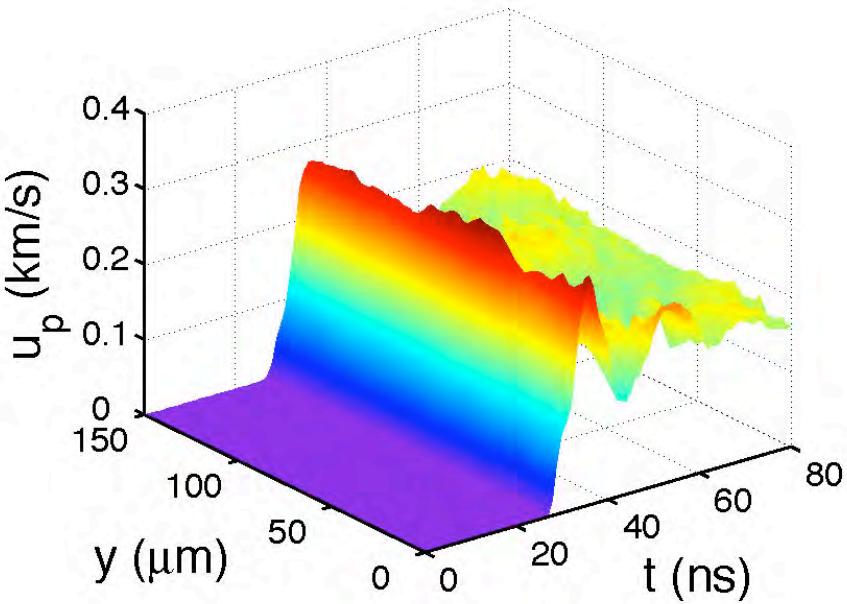

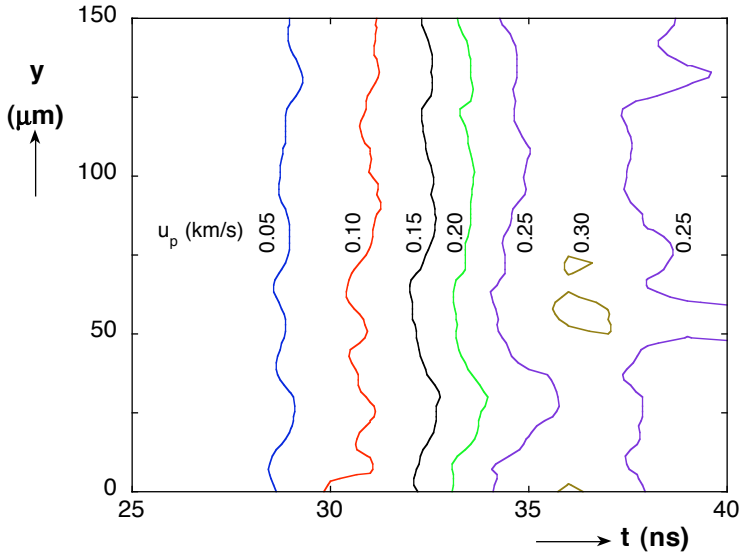

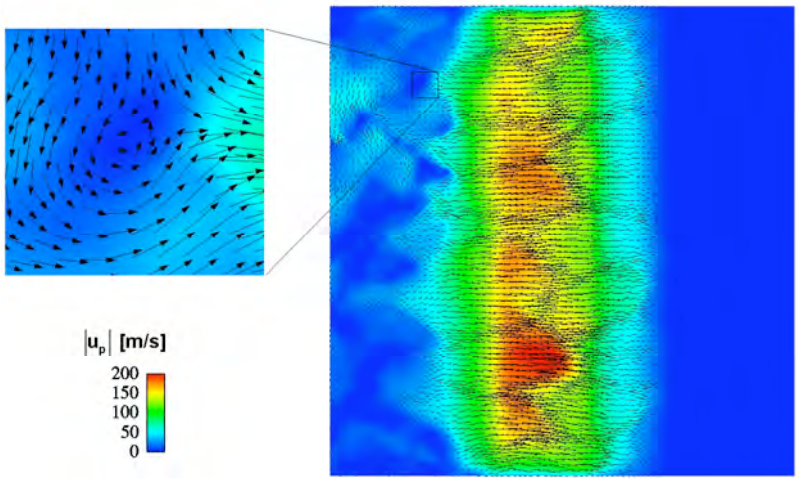

- velocity fluctuations spaced 10-30 microns
- roughness in shock front contours on order of grain size
- vortical velocity flow fields appear in wake of unloading waave

Model results: collective

I	axial	350 m/s
II	trans-1	350 m/s
III	trans-2	250 m/s
IV	trans-2	350 m/s
V	trans-1	450 m/s

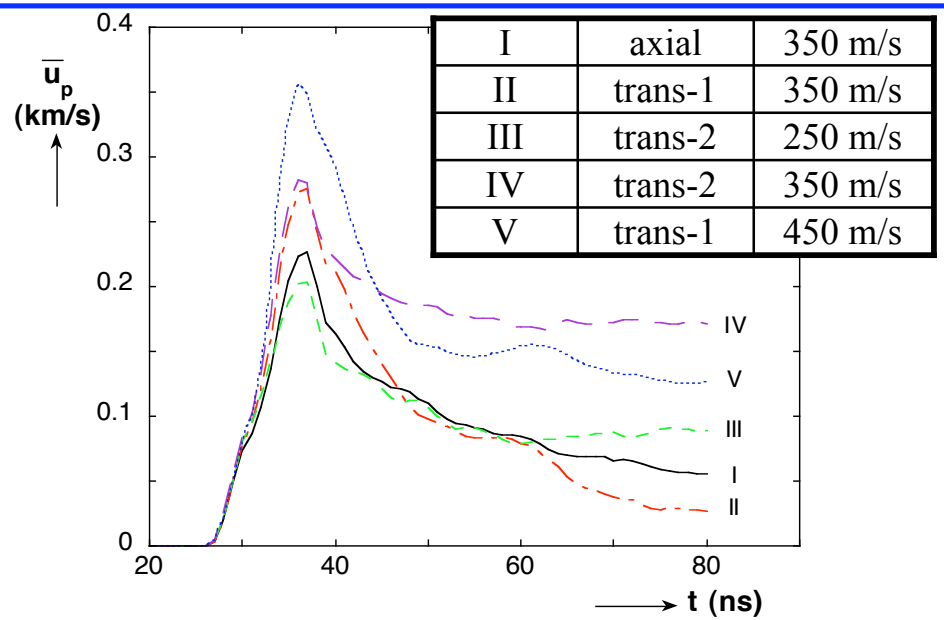

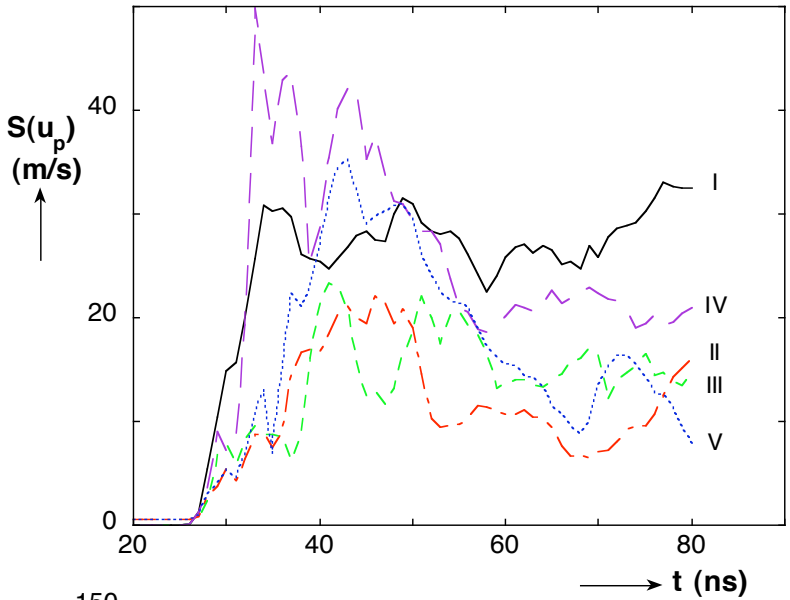

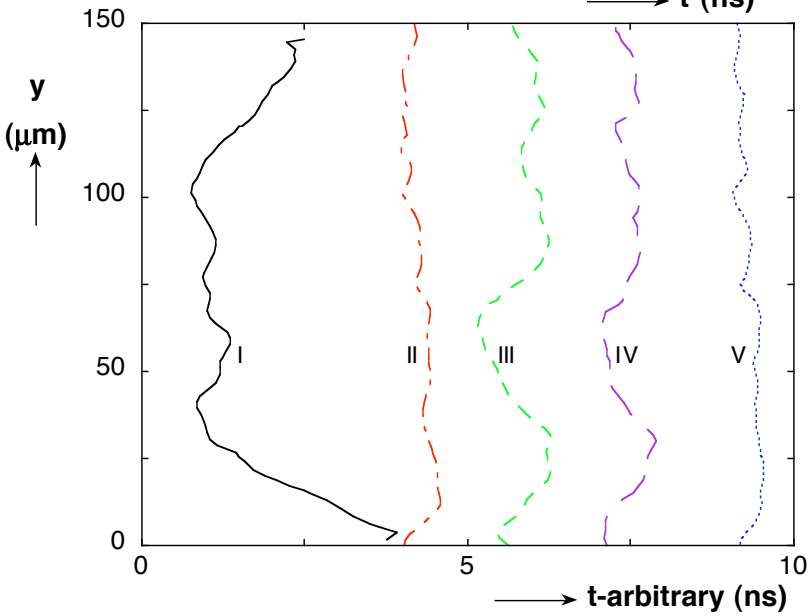

- residual velocity highest for trans-2
- no pronounced peak in deviations
- higher velocities give higher deviations
- trans-1 (equiaxed) gives lowest deviations and most uniform shock front
- ratio of roughness for 250 & 350 m/s (III and IV / trans-2) is 0.65
- ratio for axial (I) and trans-2 (IV) is 0.71

Field Variables of Model

WHA-III (trans-2, V_l = 250 m/s, t = 40 ns)

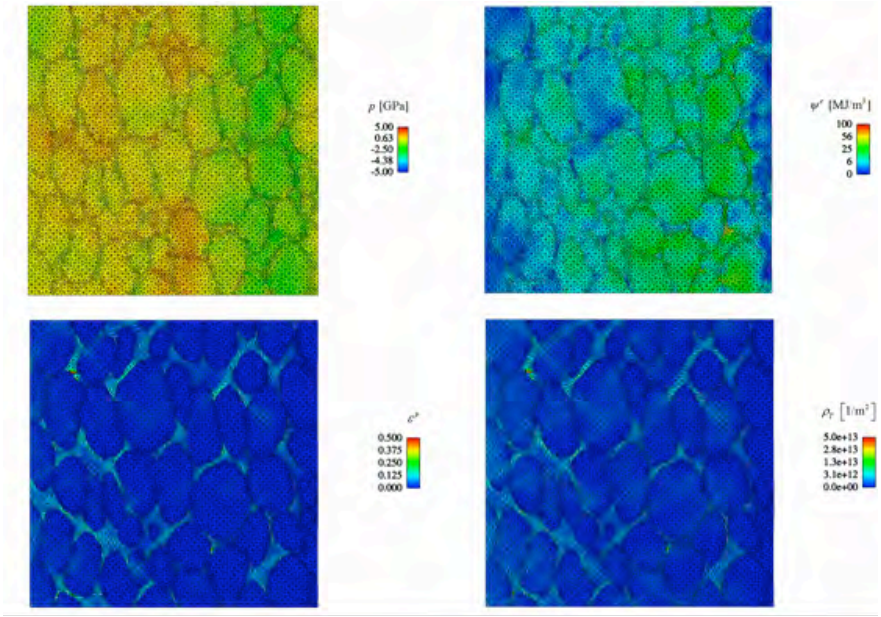

WHA-IV (trans-2, V_l = 350 m/s, t = 40 ns)

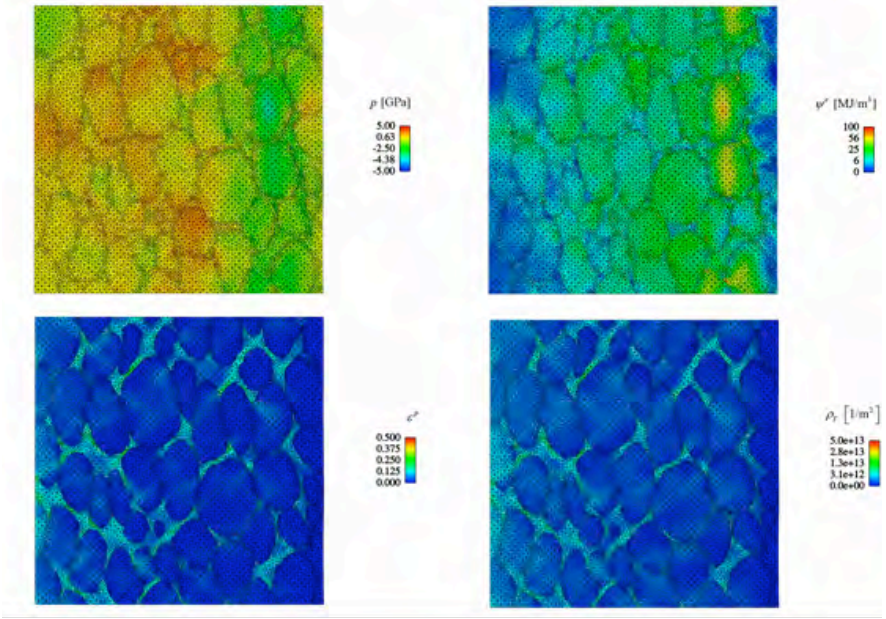

- pressure, elastic energy, plastic strain, dislocations all increase with impact velocity
- momentum conservation prevents concentration of pressure in grains vs. matrix
- strain and dislocations accumulate in matrix, local plastic strain rates reach ~10^7 s^{-1}
- deviatoric stress concentrates in stiff W grains (right, simulation WHA-IV, t = 20 ns)

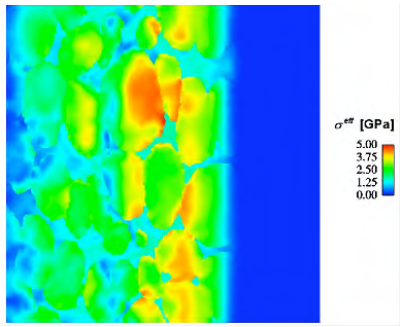

Model results: spall fracture

Effective stress at spall planes, t = 80 ns

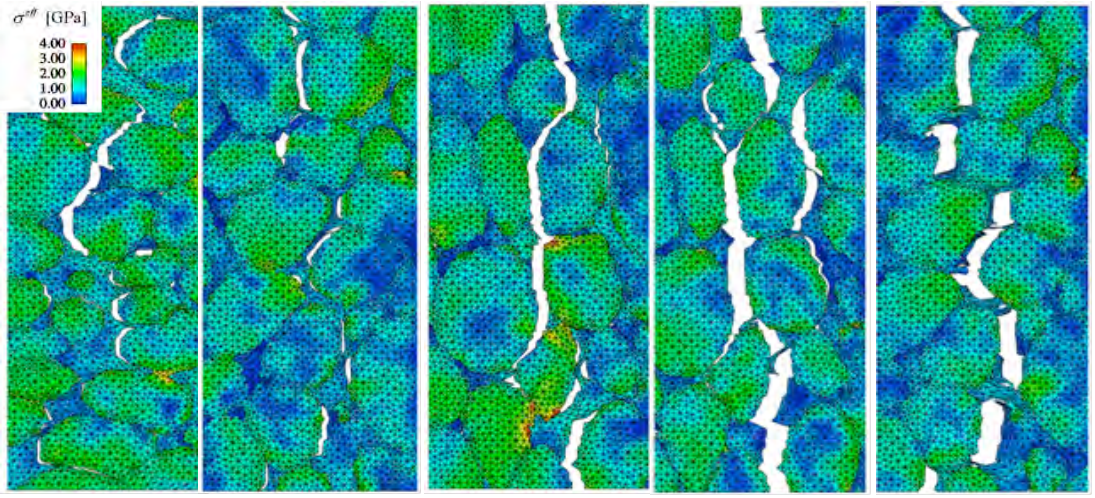

I II III IV V

			σ	β
I	axial	350 m/s	2.01	8.7
II	trans-1	350 m/s	2.88	18.8
III	trans-2	250 m/s	1.57	11.3
IV	trans-2	350 m/s	1.50	7.8
V	trans-1	450 m/s	2.69	14.9

- failure surface more torturous for axial and trans-1
- "spall strength" decreases with increased impact velocity
- trans-2 orientation has lowest "spall strength" since it presents the greatest GB area perpendicular to tensile loading
- ligaments remain since failure can only occur on W grain boundaries
- differences among microstructures not distinguishable by Weibull modulus
- Weibull moduli higher than in experiments - strength variability arises from both microstructure (grains and anisotropy) and flaw distributions

Comparison of results

Noteworthy observations

- heterogeneous wave profiles observed in both simulations and experiments
- fluctuations of 10-30 microns in simulations (grain size) and ~500 microns in experiments (several grains)
- shock roughness affected by velocity and morphology in about the same way for experiments and simulations
- deviations of 10-30 m/s for simulations, ~10 m/s for experiments
- spike in deviations seen in experiment; absent in simulation
- spall strengths lower for grains elongated perpendicular to loading direction
- deviations in spall strengths ~0.2 GPa for simulations and ~0.3-0.4 GPa for experiments
- Weibull moduli higher for simulations than experiments
- higher velocities give larger spall strengths in experiments, but not in simulations

Conclusions

- shock roughness decreases with increased velocity and is higher for transverse orientations (expt. and sim.)
- velocity deviations increase with velocity but not affected by orientation (expt.) or are lower for equiaxed grains (sim.); magnitudes are similar for expt. and sim.
- spall strength lowest for orientations with elongated grains perpendicular to loading (expt. and sim.), supporting hypothesis that failure controlled by W grain boundaries
- β higher for sim. than for expts., indicating that β is controlled by microstructure/anisotropy and nonuniform flaw distributions; no strong correlation with velocity or orientation
- proper method for comparison of model and experiments remains unclear, but standard deviation of velocity, shock front roughness, and Weibull modulus show promise

Future Work

- verify repeatability of behavior and statistics
- determine effect of measurement resolution
- investigate effect of variations in geometry
- experimental validation of plastic flow rules at higher rates

- larger domain for calculations
- multiple realizations
- 3-D simulations
- transgranular fracture criteria
- shock-induced grain boundary strengthening